

Accretion disk onto boson stars: a way to supplant black holes candidates

F. Siddhartha Guzmán

Instituto de Física y Matemáticas, Universidad Michoacana de San Nicolás de Hidalgo. Edificio C-3, Cd. Universitaria. C. P. 58040 Morelia, Michoacán, México.

The emission spectrum from a simple accretion disk model around a compact object is compared for the cases of a black hole (BH) and a boson star (BS) playing the role of the central object. It was found in the past that such a spectrum presents a hardening at high frequencies; however, here it is shown that the self-interaction and compactness of the BS have the effect of softening the spectrum, the less compact the star is, the softer the emission spectrum at high frequencies. Because the mass of the boson fixes the mass of the star and the self-interaction the compactness of the star, we find that, for certain values of the BS parameters, it is possible to produce similar spectra to those generated when the central object is a BH. This result presents two important implications: (i) using this simple accretion model, a BS can supplant a BH in the role of compact object accreting matter, and (ii) within the assumptions of the present accretion disk model we do not find a prediction that could help distinguish a BH from a BS with appropriate parameters of mass and self-interaction.

PACS numbers: 97.10.Gz 04.40.-b 04.70.-s 98.35.Jk

Since boson stars (BSs) were found to be stationary solutions of the Einstein-Klein-Gordon (EKG) system of equations [1, 2] there have been two approaches for their study in astrophysical grounds: i) proof their existence through measurable predictions and ii) use BSs as toy models for problems requiring an exotic matter component. Within the first aim some topics have been developed: prediction of particular signatures in gravitational wave emission of perturbed boson stars [3, 4, 5, 6]; prediction of differences in the emission spectrum in accretion disks around supermassive BSs vs that from BHs [7, 8, 9]. The second line of research involves proposing gigantic BSs as galactic dark halos [10, 11, 12, 13]; BSs as alternative to MACHOS [14] and BSs as solutions of tensor-scalar theories [15, 16, 17]. Around these two fronts the understanding of BSs has been widely developed, and the most important results can be found in two recent reviews by Jetzer [18] and Schunck and Mielke [19]. In this manuscript we focus on the first approach, and try to provide a picture of the properties that make a BS look like a BH, which we consider to be important because observations are at the verge of proving -or not- that black hole candidates (BHCs) have a horizon or not and when such debate involves BSs [9, 20, 21]. Firstly we present the fundamentals on Boson Stars as follows.

Boson stars are stationary solutions of Einstein's equations $G_{\mu\nu} = 8\pi GT_{\mu\nu}$, where $T_{\mu\nu} = \frac{1}{2}[\partial_\mu\phi^*\partial_\nu\phi + \partial_\mu\phi\partial_\nu\phi^*] - \frac{1}{2}g_{\mu\nu}[\phi^{*,\alpha}\phi_{,\alpha} + V(|\phi|^2)]$ is the stress-energy tensor of a complex scalar field ϕ , $g_{\mu\nu}$ is the metric of the space-time and V is the potential of the field, which for the present case is restricted to have the form $V(|\phi|) = \frac{1}{2}m^2|\phi|^2 + \frac{\lambda}{4}|\phi|^4$ where m is the mass of the field and λ its self-interaction. Whether or not the scalar field plays the role of a fundamental spinless particle, one can always consider it appears in an effective theory with lagrangian density $\mathcal{L} = -\frac{R}{16\pi G} + g^{\mu\nu}\partial_\mu\phi^*\partial_\nu\phi + V(|\phi|)$. This mean field approach helps at avoiding the formulation of

quantum field theory in a curved background.

Although axi-symmetric BS solutions have been found, we restrict here to the spherically symmetric case and choose the line element of space-time in Schwarzschild coordinates to be $ds^2 = -\alpha(r)^2dt^2 + a(r)^2dr^2 + r^2d\Omega^2$. Assuming the field to have a time dependence $\phi(r, t) = \phi_0(r)e^{-i\omega t}$ the stress energy tensor is time independent, which implies that the space-time is stationary and therefore that the metric functions α and a depend only on the radial coordinate r . Under this assumptions the Einstein-Klein-Gordon equations are:

$$\frac{a'}{a} = \frac{1-a^2}{2r} + \frac{r}{2} \left[\phi_0^2 \frac{a^2}{\alpha^2} + \phi_0'^2 + a^2(\phi_0^2 + \frac{1}{2}\Lambda\phi_0^4) \right] \quad (1)$$

$$\frac{\alpha'}{\alpha} = \frac{a^2-1}{r} + \frac{a'}{a} - ra^2\phi_0^2(1 + \frac{1}{2}\Lambda\phi_0^2) \quad (2)$$

$$\phi_0'' + \phi_0' \left(\frac{2}{r} + \frac{\alpha'}{\alpha} - \frac{a'}{a} \right) + \phi_0 \frac{a^2}{\alpha^2} - a^2(1 + \Lambda\phi_0^2)\phi_0 = 0 \quad (3)$$

where we have used the rescaled variables $\phi_0 \rightarrow \sqrt{4\pi G}\phi_0$, $r \rightarrow mr$, $t \rightarrow \omega t$, $\alpha \rightarrow \frac{m}{\omega}\alpha$ and $\Lambda = \frac{\lambda}{4\pi Gm^2}$; primes indicate derivative with respect to the radial coordinate. The system (1-3) is a set of coupled ordinary differential equations to be solved under the conditions $a(0) = 1$, $\phi_0(0)$ finite and $\phi_0'(0) = 0$ in order to guarantee regularity and spatial flatness at the origin, and $\phi_0(\infty) = \phi_0'(\infty) = 0$ in order to ensure asymptotic flatness at infinity as described in [1, 22, 23, 24, 25]; these conditions reduce the system (1-3) to an eigenvalue problem for ω . The solution was calculated numerically using finite differencing and a shooting routine that searched ω .

The solutions to this set of equations define sequences of equilibrium configurations like those shown in Fig. 1(a). In the curves two important points for each value of Λ are marked: i) the critical point -marked with a filled circle- indicating the threshold between the stable

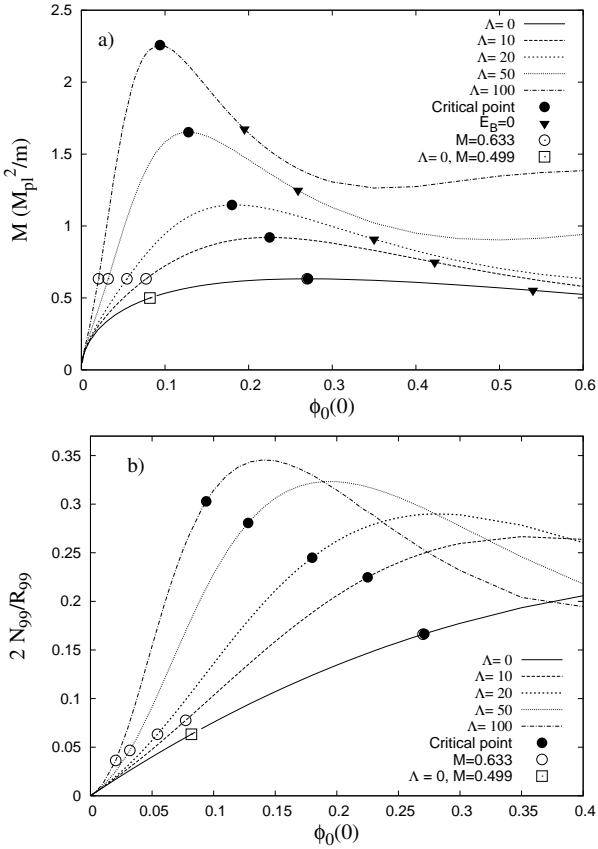


FIG. 1: (a) Sequences of equilibrium configurations for different values of Λ are shown as a function of the central value of the scalar field $\phi_0(0)$. The circles indicate the critical point that divides the stable from the unstable solutions. The inverted triangles indicate the point at which the binding energy is zero. Those configurations between the circles and the triangles (along each sequence) collapse into black holes even under infinitesimal perturbations (see [27] for the full tracking of the formation of an event horizon out of an unstable boson star). Configurations to the right of the triangles disperse away. (b) The compactness of each solution is shown. The critical point is also marked, since the interesting configurations would be those boson stars that are stable (to the left of the circles). In both plots, the transparent circles indicate the special set of configurations we calculate the emission spectrum for in what follows; in the case of $\Lambda = 0$ such configuration is very close to the critical point and it is difficult to look at, but it is in there. The configuration marked with a square corresponds to a configuration with $\Lambda = 0$, $M = 0.499$ and compactness 0.06332; this compactness is the same as that of configuration with $\Lambda = 20$ and $M = 0.633$, see text below to take advantage of this remark.

and unstable branches of each sequence, that is, configurations to the left of this point are stable and those to the right are unstable as found through the analysis of perturbations [24, 25], catastrophe theory [26] and full non-linear evolution of the evolution equations [22, 23] and ii) the point at which the binding energy $E_B = M - Nm = 0$ marked with an inverted filled triangle,

where $N = \int j^0 d^3x = \int \frac{i}{2} \sqrt{-g} g^{\mu\nu} [\phi^* \partial_\nu \phi - \phi \partial_\nu \phi^*] d^3x$ is the number of particles and $M = (1 - 1/a^2)r/2$ evaluated at the outermost point of the numerical domain is the Schwarzschild mass; the configurations between the instability threshold and the zero binding energy point collapse into black holes whereas those to the right disperse away as shown in [27]. The units for the M and N are given in M_{pl}^2/m , where M_{pl} is the Planck mass and m is the mass of the boson.

Since the mass of the configurations in Fig. 1(a) scales with m , the original use of the self-interaction Λ was to allow bigger masses even if the mass parameter m was fixed [28] and thus BS configurations seemed to be -gravitationally- similar to compact objects like neutron stars [28]. In the present approach neither m nor Λ will be considered related to any type of possibly existing particle, instead they are thought of as free parameters that permit faking compact objects. We prefer to focus on another property of BSs: the compactness. In Fig. 1(b) the compactness of equilibrium configurations is shown. Provided BSs have no defined surface we consider that the radius containing 99% (R_{99}) of the total particle number (following [22, 23] where 95% was considered instead) is a reasonable place where to measure the gravitational field of the star; thus the compactness plotted in Fig. 1(b) is defined as $2N_{99}/R_{99}$, where N_{99} is the number of particles integrated up to R_{99} . One could feel tempted to believe that the more compact a BS is more similar to a BH seems, however as shown below this happens only in terms of how deep the trajectories of test particles can be.

Time-like geodesics. Given the line element $ds^2 = -\alpha(r)^2 dt^2 + a(r)^2 dr^2 + r^2 d\Omega^2$, the equation for time-like geodesics followed by test particles on the equatorial plane reads:

$$\dot{r}^2 + \frac{1}{a^2} \left(1 + \frac{L^2}{r^2} \right) = \frac{E^2}{\alpha^2 a^2}, \quad (4)$$

where $L^2 = r^4 \dot{\varphi}^2$ and $E^2 = -\alpha^2 t^2$ are the squared angular momentum and energy at spatial infinity, which are the conserved quantities of the test particle related to the independence on the azimuthal angle φ and t of the space-time respectively; an overdot indicates derivative with respect to the proper time of the test particle. The geodesics for a Schwarzschild BH are given by (4) with the values $\alpha^2 = a^{-2} = (1 - \frac{2M}{r})$. Since equation (2) for α is linear, we rescale this function so that at infinity $\alpha(r \rightarrow \infty) = 1/a(r \rightarrow \infty)$, thus at infinity $\alpha^2 = a^{-2}$, which implies the coefficient of E^2 in (4) is one for BSs, which also happens for the BH.

At this point it is convenient to draw the effective potential $V_{eff}^2 = \frac{1}{a^2} \left(1 + \frac{L^2}{r^2} \right)$ for a given angular momentum of the test particle. In Fig. 2 we show V_{eff}^2 for different values of L and compare with the potentials due to a BH. It happens that the effective potentials for a BS

depend on the compactness of the star only and are independent of the self-interaction; instead of showing this fact we present the potentials for configurations with the same mass ($M = 0.633(M_{pl}^2/m)$) and $\Lambda = 0, 20$ with compactness 0.1666 and 0.06332 respectively. The location of the typical potential barrier for test particles on a BS space-time [5, 7, 29] changes from one case to the other: the less compact the star ($\Lambda = 20$) the farther the location of the barrier from the center.

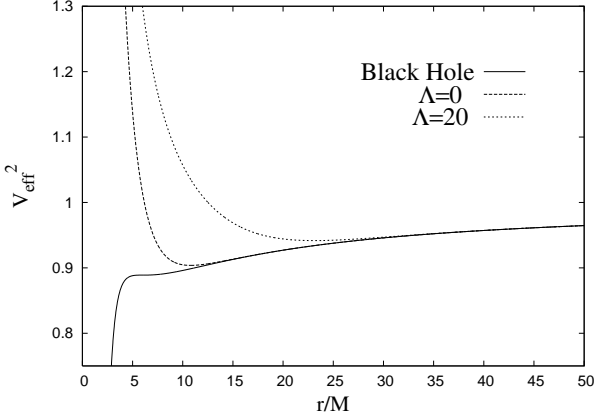


FIG. 2: Here it is shown the effective potential that a particle with $L^2 = 12M^2$ “feels” for two configurations of the same mass $M = 0.633$ and $\Lambda = 0, 20$, and for a black hole of the same mass. At $r = 6M$ it is possible to see the ISCO for a test particle on a BH space-time. The interesting result is that for the more compact stars test particles can travel deeper inside the star. What is possible to infer is that freely falling observers cannot distinguish whether there is a BH or a BSs from $r = 30M$ on.

It is known that BSs admit stable circular orbits for every radius [8]. Thus, here we do not touch that problem and restrict to calculate E and L in terms of the metric functions. In order to do so we rewrite (4) for $\dot{r} = 0$ and demand $dV/dr = 0$ with $V = [(1 + L^2/r^2) - E^2/\alpha^2]/a^2$. This condition implies

$$E = \frac{\alpha^2}{\sqrt{\alpha^2 - r\alpha\alpha'}}, \quad \& \quad L = \sqrt{\frac{r^3\alpha\alpha'}{\alpha^2 - r\alpha\alpha'}} \quad (5)$$

where $\alpha^2 - r\alpha\alpha' > 0$ all the way as shown in Fig. 3(a) for a typical BS. Before proceeding to the calculation of the emission spectrum we need the angular velocity of a test particle given by $\Omega = \sqrt{\frac{\alpha\alpha'}{r}}$, which is a regular function for all values of r . In Fig 3(b) the values of E , L and the useful $E - \Omega L$ are shown for the $M = 0.633$, $\Lambda = 20$ BS and a BH of the same mass.

The accretion disk model is that of a geometrically thin, optically thick, steady accretion disk. The power per unit area generated by such a disk rotating around a

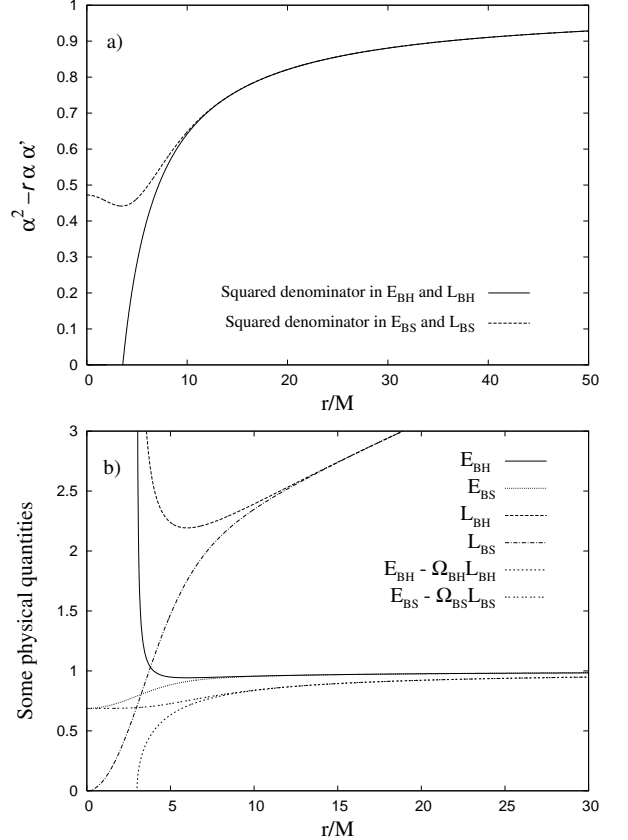


FIG. 3: a) The squared denominator of E and L in (5); the star chosen is the one with $\Lambda = 0$, central field $\phi(0) = 0.271$ and mass $M = 0.633(M_{pl}^2/m)$. b) Physical quantities used for the calculation of $D(r)$ (see below); the solid line indicates these quantities for a black hole of the same mass as the star. The results in this plot coincide with those obtained in [8].

central object is given by [8, 30]:

$$D(r) = \frac{\dot{M}}{4\pi r} \frac{\alpha}{a} \left(-\frac{d\Omega}{dr} \right) \frac{1}{(E - \Omega L)^2} \int_{r_i}^r (E - \Omega L) \frac{dL}{dr} dr \quad (6)$$

where \dot{M} is the accretion mass rate and r_i is the inner edge of the disk, keeping in mind that r is in units of $1/m$. For black holes this radius is assumed to be at the ISCO ($r = 6M$) of the hole. Since BSs allow circular orbits in the whole spatial domain we consider that $r_i = 0$ for BSs. Furthermore, assuming it is possible to define a local temperature we use the Steffan-Boltzmann law so that $D(r) = \sigma T^4$, where $\sigma = 5.67 \times 10^{-5} \text{ erg s}^{-1} \text{ cm}^{-2} \text{ K}^{-4}$ is the Steffan-Boltzmann constant. Now, considering the disk emits as a black body, we use the dependence of T on the radial coordinate and therefore the luminosity $L(\nu)$ of the disk and the flux $F(\nu)$ through the expression for the black body spectral distribution:

$$L(\nu) = 4\pi d^2 F(\nu) = \frac{16\pi h}{c^2} \cos(i) \nu^3 \int_{r_i}^{r_f} \frac{r dr}{e^{h\nu/kT} - 1} \quad (7)$$

where d is the distance to the source, r_i and r_f indicate the location of the inner and outer edges of the disk, $h = 6.6256 \times 10^{-27} \text{ erg s}$ is the Planck constant and $k = 1.3805 \times 10^{-16} \text{ erg K}^{-1}$ is the Boltzmann constant and i is the disk inclination. The algorithm to construct the emission spectrum for such a model of accretion disk around a BS and a BH is as follows:

- 1) Define the space-time functions a and α by choosing one of the equilibrium configurations in Fig. 1 and calculate M .
- 2) Define the metric of the equivalent BH through $\alpha_{BH} = \sqrt{1 - 2M/r}$ and $a_{BH} = 1/\sqrt{1 - 2M/r}$.
- 3) Calculate the angular velocity, angular momentum and energy of a test particle for both space-times $\Omega_{BS,BH}$, $L_{BS,BH}$, $E_{BS,BH}$.
- 4) Use such quantities to calculate the power emitted in both cases $D_{BS}(r)$ and $D_{BH}(r)$ defined in (6).
- 5) Calculate the temperature of the disk in both cases $T_{BS}(r) = (D_{BS}(r)/\sigma)^{1/4}$ and $T_{BH}(r) = (D_{BH}(r)/\sigma)^{1/4}$.
- 6) Use such temperature to integrate the luminosity (7) $L_{BS}(\nu)$ and $L_{BH}(\nu)$ for several values of ν .

We choose a configuration with $M = 0.633(M_{pl}^2/m)$ because it has been used in the past (e.g. [8]), but it could be any other; the usual reason to use this configuration is that for $\Lambda = 0$ it corresponds to the most compact configuration in the stable branch (see Fig. 1). We take the physical parameters used in [8], where $m = 1.2 \times 10^{-25} \text{ GeV}$, $\dot{M} = 0.633(M_{pl}^2/m) = 2.8 \times 10^6 M_\odot$, $i = 60^\circ$, which we use here too. We used $r_f = 30$ and $50M$ and found no qualitative difference in the spectrum. As a test in the present calculations we show here the results found in [8] for such system in Fig. 4 as a particular case, which is interpreted as a possible signature of BSs because there is a hardening of the spectrum at high frequencies.

Nevertheless, what we do here is to repeat our algorithm for the same mass of the object but different values of Λ keeping the same value of the mass (the configurations marked with simple circles in Fig. 1). The result can be found in Fig. 4, where the spectrum is softened when increasing Λ , in fact we notice that for $\Lambda = 20$ the spectrum could perfectly be that of the equivalent black hole; we dub this particular configuration the Star Y and remark its compactness $2M_{99}/R_{99} = 0.06332$. Under the present model of accretion disk it would be rather difficult to distinguish between a black hole and a boson star with mass $M = 2.8 \times 10^6 M_\odot$ under the parameters $m = 1.2 \times 10^{-25} \text{ GeV}$ and $\Lambda = 20$ compared with the case $\Lambda = 0$ where $\nu L(\nu)$ is orders of magnitude bigger for the BS than for the BH around the 10^{16} Hz window.

Once the algorithm is settled down we try one last experiment: we choose a $\Lambda = 0$ star with the same compactness as that of star Y , such configuration appears in Fig. 1 marked with a square. The mass of such star is $M = 0.499(M_{pl}^2/m)$; in order to achieve a

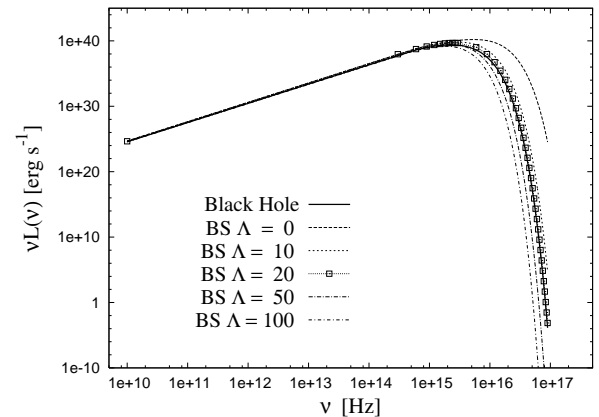


FIG. 4: The emission spectrum from a central star with mass $M = 0.633(M_{pl}^2/m)$ and different values of Λ . The solid line is obtained when a black hole is considered as the central object. The curve for $\Lambda = 0$ coincides with the one obtained in [8] and shows the hardening of the spectrum at high frequencies. The case $\Lambda = 20$ is particularly interesting because it seems to match the spectrum obtained with the BH.

mass equal to that of configurations of Fig. 4 we need to use $m = 0.499/0.633 \times 1.2 \times 10^{-25} \text{ GeV}$. The resulting spectrum is shown in Fig. 5 where once again it is possible to nearly match the spectrum corresponding to that of a BH with the same mass, but this time without the need of self-interaction.

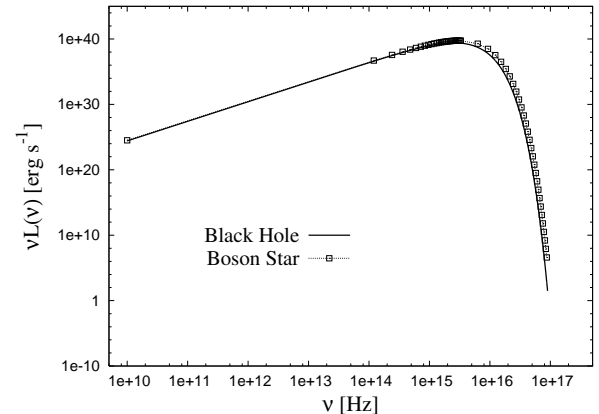


FIG. 5: The emission spectrum from a disk with a central star with mass $M = 0.499(M_{pl}^2/m)$ and $\Lambda = 0$. In order to keep M equal to that of configurations in Fig. 4 it is necessary to set $m = 0.499/0.633 \times 1.2 \times 10^{-25} \text{ GeV}$, otherwise we could construct a correct spectrum with the incorrect gravitational mass. The similarity between the spectrum due to the BS and to the BH is not as impressive as that of the Star Y , but the hardening of the spectrum is not as strong as that of $\Lambda = 0$ in the previous plot. We simply used a star with no self-interaction and compactness $2M_{99}/R_{99} = 0.06332$ as that of Star Y .

Discussion and conclusions. There are two main

results: 1) BSs can play the role of BHCs and 2) the emission spectrum is not helpful at determining whether or not the BHC is a BS or a BH and in consequence it is not enough to say whether the compact object has a horizon or not within the accretion model of the present approach. There are two ways of faking the spectrum of the disk around a BH: i) by using an appropriate value of Λ for a given m and ii) by using an appropriate value of m with $\Lambda = 0$.

We expect the results presented here are disk model dependent, however the study of other different accretion disk models could show a similar behavior. Nevertheless, at this point one can conclude that the spectrum is not enough to determine whether a compact object is a BS or not, and in any case m and Λ remain free parameters that could help at matching an emission spectrum.

For instance, in [9] the accretion of ordinary nucleonic gas on black hole candidates is analyzed by assuming that the BHC is either a perfect fluid star or a boson star instead of a black hole. The result indicates that for such cases Type I X-ray bursts should be observed because the accreting gas particles pile up on the surface of the stars, since in both type of stars the Schwarzschild radius lies inside the star. Because such bursts are not observed, these two types of stars are ruled out as

BHCs and it is considered that the BHC is a black hole. Nonetheless, the assumption that BSs have surface is not correct and a test particle would not be subject to mechanical forces due to the presence of a surface; thus the analysis in [9] should be redone under such consideration.

Finally, it could be that under different accretion disk models, particular observable BS signatures could appear in the electromagnetic spectrum. At the same time, it is remarkable the effort invested in the prediction of BS signatures through gravitational wave signals due to particles surrounding a BS [5] and due to full 3D perturbations [6].

Acknowledgments

The author thanks Diego F. Torres and L. Arturo Ureña-López for criticism, comments and ideas. This research is partly granted by CIC-UMSNH-4.9 and PROMEP-UMICH-PTC-121. The runs were carried out in the Ek-bek cluster of the “Laboratorio de Supercomputo Astrofísico (LASUMA)” at CINVESTAV-IPN. The code was developed in hardware from the Center for Computation and Technology at Louisiana State University.

[1] R. Ruffini and S. Bonazolla, Phys. Rev. **187**, 1767 (1969).
 [2] D. J. Kaup, Phys. Rev. **172**, 1331 (1968).
 [3] S. Yoshida, Y. Eriguchi and T. Futamase, Phys. Rev. **D 50**, 6235 (1994).
 [4] F. D. Ryan, Phys. Rev. **D 55**, 6081 (1997).
 [5] M. Kesden, J. Gair and M. Kamionkowski, Phys. Rev. **D 71**, 044015 (2005).
 [6] J. Balakrishna, R. Bondarescu, G. Dauces, F. S. Guzmán and E. Seidel, Class. Quantum Grav. (submitted).
 [7] D. F. Torres, S. Capozziello and G. Lambiase, Phys. Rev. **D 62**, 104012 (2000).
 [8] D. F. Torres, Nucl. Phys. **B 26**, 377 (2002).
 [9] Y-F. Tuan, R. Narayan and M. J. Rees, ApJ **606**, 1112 (2004).
 [10] Jae-woon Lee, In-guy Koh, Phys. Rev. **D 53**, 2236 (1996).
 [11] E. W. Mielke and F. E. Schunck, Phys. Rev. **D 66**, 023503 (2002).
 [12] F. E. Schunck, PhD Thesis, University of Cologne 1996.
 [13] F. S. Guzmán and L. A. Ureña-López, Phys. Rev. **D 68** (2003) 024023. *Ibid.* Phys. Rev. **D 69**, 124033 (2004).
 [14] E. W. Mielke and F. E. Schunck, Nucl.Phys. **B564**, 185 (2000).
 [15] J. J. van der Bij and M. Gleiser, Phys. Lett **B 194**, 482 (1987).
 [16] D. F. Torres, Phys. Rev. **D 56**, 3478 (1997).
 [17] J. Balakrishna, Ph D Thesis, Washington University 1999. E-print gr-qc/9906110.
 [18] P. Jetzer, Phys. Rep. **220** 4 (1992) 163.
 [19] F. E. Schunck and E. W. Mielke, Class. Quantum Grav. **20**, R301 (2003).
 [20] M. A. Abramowicz, W. Kluzniak and J-P. Lasota, A & A **396**, L31-L34 (2002).
 [21] J. E. McClintock, R. Narayan, G. B. Rybicki, ApJ **614**, 881 (2004).
 [22] E. Seidel and W-M. Suen, Phys. Rev. **D 42**, 384 (1990).
 [23] J. Balakrishna, E. Seidel and W-M. Suen, Phys. Rev. **D 58**, 104004 (1998).
 [24] M. Gleiser, Phys. Rev. **D 38**, 2376 (1988).
 [25] S. H. Hawley and M. W. Choptuik, Phys. Rev. **D 62**, 104024 (2000).
 [26] F. Kusmartsev, E. W. Mielke and F. E. Schunck, Phys. Rev **D 43**, 3895 (1991).
 [27] F. S. Guzmán, Phys. Rev. **D 70**, 044033 (2004).
 [28] M. Colpi, S. L. and I. Wasserman, Phys. Rev. Lett. **57**, 2485 (1986).
 [29] F. S. Guzmán, J. of Physics, Conf. Series, **24**, 241 (2005).
 [30] D. Page and K. S Thorne, ApJ **191**, 499 (1974).